

## A simple model of the plane gas bubble in a finite liquid

By R. COLLINS

Department of Mechanical Engineering, University College London

(Received 11 December 1964)

Using a method due to Davies & Taylor (1950), a simple model is employed to derive the velocity of a two-dimensional gas bubble rising in liquid along the axis of a channel of finite width. The asymptotes of the solution agree well with previous results and an experimental investigation confirms the effect of channel width on bubble velocity. Measured values of velocity are, however, approximately 9% higher than theoretical values due to the three-dimensional nature of the real flow.

---

### 1. Introduction

The study of large gas bubbles rising in liquids has been recently stimulated by a remarkable analogy described by Davidson & Harrison (1963). They have shown that a bubble rising in a bed of solid particles fluidized\* by the vertical flow of gas through it, appears to behave like a gas bubble rising in a liquid. Results obtained for gas-liquid systems, such as those of Davies & Taylor (1950) relating to the spherical-capped bubble in an infinite region of liquid, and of Dumitrescu (1943) for the rise of infinitely long bubbles in tubes, can therefore be applied to the fluidized state. The establishment of the analogy relies on the application of an empirical correction, due to Uno & Kintner (1956), for the effect of a containing cylindrical boundary on bubble velocity. Since an infinitely long bubble can be regarded as being produced when the cylinder diameter becomes sufficiently small, a theoretical expression for this correction would have as its asymptotes the known solutions of Davies & Taylor and of Dumitrescu. The complexity of the latter's solution appears to eliminate the possibility of finding an exact theoretical expression linking these two limits. It is possible, however, to generate an approximate solution for the two-dimensional problem using the method of Davies & Taylor. This problem is of interest because two-dimensional beds have been used extensively in fluidization studies. In applying Davidson's (1961) model of the fluidization bubble to finite beds, Collins (1965) has shown that, under certain conditions, a single bubble on the axis of a finite bed can capture all of the gas flowing into the bed. The solution of the problem considered here is necessary in order to calculate bubble sizes capable of producing this phenomenon.

\* The object of the fluidization process, which is widely used in the chemical engineering industry, is to obtain intimate contact between gas and solid in order to promote heat transfer, mass transfer, or catalytic reaction. A study of bubble behaviour is necessary to determine how the efficiency of the process is affected by their appearance.

With the assumptions that viscous and surface-tension forces are insignificant in comparison with inertia forces, and that the gas pressure is constant within the bubble, several theoretical results are known. Applying Bernoulli's equation to the streamline forming the bubble boundary, it is found that the constant-pressure condition is satisfied if the velocity  $q$  at a point on the boundary a vertical distance  $s$  below the front stagnation point is given by

$$q^2 = 2gs, \quad (1)$$

where  $g$  is the acceleration due to gravity. A complete analysis would give the bubble boundary as part of the solution, but in both two dimensions and three dimensions this presents a considerable problem. Davies & Taylor neatly avoided this difficulty. In their method the bubble velocity was taken to be that which satisfied equation (1) only at the front stagnation point, and they assumed that the flow in that region was described by the irrotational flow past a sphere having the same curvature. This approach gave the velocity of a spherical-capped bubble in an infinite liquid as

$$U_\infty = \frac{2}{3}(ga)^{\frac{1}{2}}, \quad (2)$$

where  $a$  is the radius of curvature at the front stagnation point. Davies & Taylor showed experimentally that equation (2) relates  $U$  and  $a$  very well for large air bubbles in water and nitrobenzene. The corresponding result for the plane bubble was not derived in their paper but may be shown to be

$$U_\infty = 0.5(ga)^{\frac{1}{2}}. \quad (3)$$

Davies & Taylor also gave an approximate result for the velocity of an infinitely long bubble in a fluid contained within a circular tube, but Dumitrescu's analysis is usually considered a better approximation. He gave

$$U_s = 0.495(gb)^{\frac{1}{2}}, \quad (4)$$

where  $b$  is the tube radius. Nicklin, Wilkes & Davidson (1962) have shown empirically that once a bubble in a tube is longer than about one tube diameter, its velocity is independent of its length and is given by equation (4). Such bubbles are called slugs. Slugs of differing lengths are found to have geometrically similar caps and the ratio  $a/b$  approaches a constant limiting value less than unity. The equivalent plane case was discussed by Garabedian (1957) who derived

$$U_s = 0.337(gb)^{\frac{1}{2}}, \quad (5)$$

while Birkhoff & Carter (1956) gave a constant of  $0.33 \pm 0.01$ . By analogy with the three-dimensional case, equation (5) is expected to apply to the plane slug, and equations (3) and (5) should thus be the asymptotes of the two-dimensional solution.

## 2. The model

Consider the flow system shown in figure 1 (*a*), which will be taken to model the flow over the bubble shown in figure 1 (*b*). Axes are fixed on the cylinder which rises with velocity  $U$ . Lamb's (1932) equation for the complex potential of the

flow of a uniform stream past a nearly circular body in a channel may be written in the modified form

$$w = U \left[ z + \frac{2b}{\pi} \sinh^2 \frac{\pi c}{2b} \coth \frac{\pi z}{2b} \right], \tag{6}$$

where  $z = x + iy$ , and the function  $(2b/\pi) \sinh^2(\pi c/2b)$  ensures that the body is of length  $2c$  for all values of  $c/b$ . The streamline  $\psi = 0$  enclosing the body has the equation

$$z - \bar{z} + \frac{2b}{\pi} \left[ \coth \frac{\pi z}{2b} - \coth \frac{\pi \bar{z}}{2b} \right] \sinh^2 \frac{\pi c}{2b} = 0, \tag{7}$$

where a bar denotes the complex conjugate, and it is remarkably circular for values of  $c/b$  from zero to approximately 0.5. Equation (7) also contains the real axis  $z = \bar{z}$  as one root.

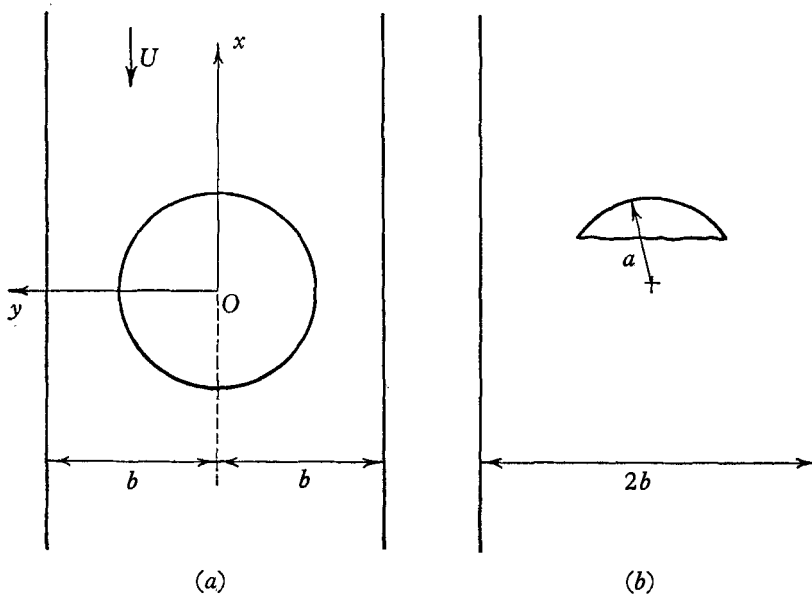


FIGURE 1. The flow model of the cylindrical-capped bubble in a channel.

The radius of curvature  $a$  of the body at its front stagnation point may be derived from equation (7) as

$$\frac{a}{c} = \frac{6b \tanh(\pi c/2b)}{\pi c [3 - \tanh^2(\pi c/2b)]}. \tag{8}$$

Figure 2 reveals that, until  $c/b$  exceeds 0.4, the radius of curvature  $a$  is sensibly constant and equal to  $c$ , and further, that for values of  $c/b > 2$ ,  $a/b = 3/\pi = 0.955$ .

In complex-variable terms, the condition for constant pressure becomes

$$q^2 = g(2c - z - \bar{z}), \tag{9}$$

and from equation (6)

$$q^2 = \left[ \frac{dw}{dz} \right] \left[ \frac{d\bar{w}}{d\bar{z}} \right] = U^2 \left[ 1 - \sinh^2 \frac{\pi c}{2b} \operatorname{cosech}^2 \frac{\pi z}{2b} \right] \left[ 1 - \sinh^2 \frac{\pi c}{2b} \operatorname{cosech}^2 \frac{\pi \bar{z}}{2b} \right], \tag{10}$$

where, in both equations,  $z$  and  $\bar{z}$  are related by equation (7). Using the method of Davies & Taylor, the rise velocity is determined by

$$U^2 = \lim_{z \rightarrow c} \frac{g(2c - z - \bar{z})}{[1 - \sinh^2(\pi c/2b) \operatorname{cosech}^2(\pi z/2b)][1 - \sinh^2(\pi c/2b) \operatorname{cosech}^2(\pi \bar{z}/2b)]}, \quad (11)$$

where the limit is approached along the bubble boundary given in equation (7). It is convenient to write equation (6) as

$$w = Ut(z), \quad (12)$$

so that equation (7) becomes

$$t(z) - t(\bar{z}) = 0, \quad (13)$$

which may be expressed in the alternative form

$$\bar{z} = f(z). \quad (14)$$

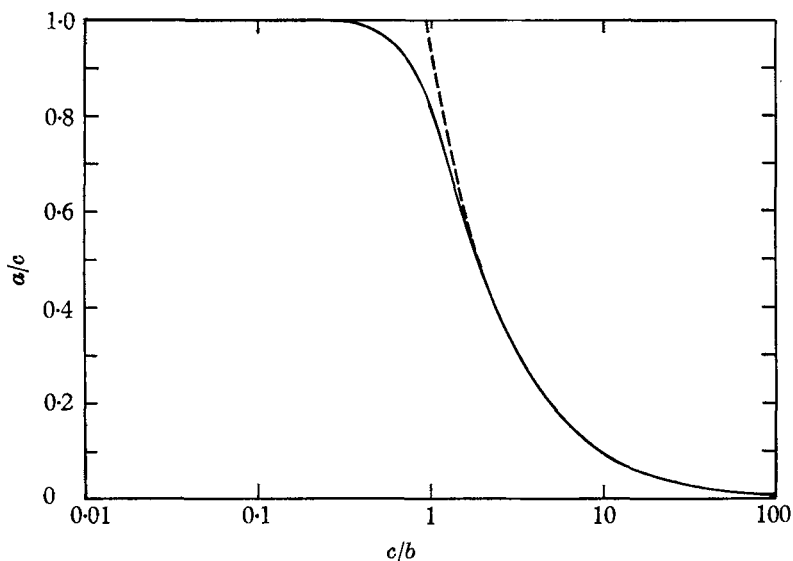


FIGURE 2. The radius of curvature at the front stagnation point of the model. - - - -,  $a/c = 3b/\pi c$ ; —, equation (8).

Denoting differentiation with respect to the argument of a function by a prime, equation (10) becomes

$$q^2 = U^2 [t'(z)]^2 / f'(z), \quad (15)$$

and equation (11) may thus be written as

$$U^2 = \lim_{z \rightarrow c} \frac{g[2c - z - f(z)]f'(z)}{[t'(z)]^2}. \quad (16)$$

The limit is evaluated by expanding the functions appearing in it about the front stagnation point. Since  $f(c) = c$ ,  $t'(c) = 0$  and  $f'(c) = -1$  evaluated along the closed branch of the zero streamline, it is found that

$$U^2 = \frac{1}{2} \left[ \frac{gf''}{(t'')^2} \right]_c. \quad (17)$$

Manipulation of equations (13) and (14), involving the evaluation of a further limit, gives

$$f''(c) = -\frac{2}{3} \left[ \frac{t'''}{t''} \right]_c, \tag{18}$$

so that

$$U^2 = -\frac{g}{3} \left[ \frac{t'''}{(t'')^3} \right]_c. \tag{19}$$

Evaluation of  $t'''(c)$  and  $t''(c)$  for the chosen model produces

$$U = \sqrt{\left( \frac{gb}{6\pi} \left[ 3 - \tanh^2 \frac{\pi c}{2b} \right] \tanh \frac{\pi c}{2b} \right)}. \tag{20}$$

From this equation it can be seen that, as  $c/b \rightarrow 0$ ,  $U \rightarrow U_\infty = 0.5(ga)^{\frac{1}{2}}$ , and that as  $c/b \rightarrow \infty$ ,  $U \rightarrow U_s = (gb/3\pi)^{\frac{1}{2}} = 0.326(gb)^{\frac{1}{2}}$ . Thus the solution agrees well with

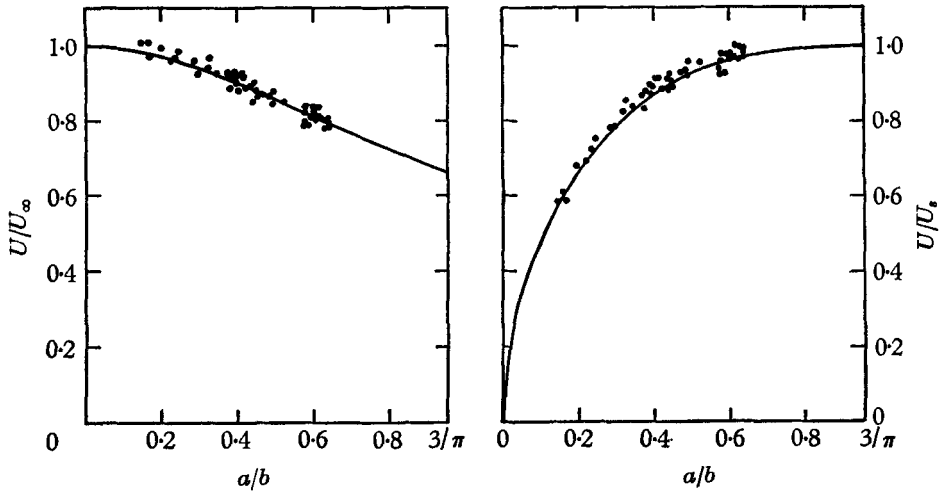


FIGURE 3. Variation of bubble velocity with  $a/b$ .

the required asymptotes, the result for the slug being less than 3.5 % below Garabedian's and falling within the range of error of that due to Birkhoff & Carter. It is rather surprising that such a simple model agrees with the slug limit for it certainly does not describe the flow away from the stagnation point when the bubble is very long. It gives an almost constant velocity near the walls whereas, for the true boundary, the fluid should be falling freely there.

The parameter  $c$  may be eliminated from equations (8) and (20) to give

$$\frac{U}{U_s} = \sqrt{\left( \frac{3b}{\pi a} \left[ 3 + \left( \frac{3b}{\pi a} \right)^2 \right] \right) - \left( \frac{3b}{\pi a} \right)^{\frac{3}{2}}}, \tag{21}$$

or

$$\frac{U}{U_\infty} = \frac{2b}{\pi a} \sqrt{\left[ 3 + \left( \frac{3b}{\pi a} \right)^2 \right] - 6 \left( \frac{b}{\pi a} \right)^2}, \tag{22}$$

where  $U_s = (gb/3\pi)^{\frac{1}{2}}$  and  $U_\infty = 0.5(ga)^{\frac{1}{2}}$ . Equations (21) and (22) are plotted in figure 3 together with points obtained from experiments with air bubbles rising through water.

### 3. Experiments

The apparatus, shown in figure 4, consisted of two acrylic plates  $\frac{3}{8}$  in. thick and 3 ft. square separated by rubber-covered spacers,  $\frac{1}{4}$  in. thick. The edges were sealed and distortion of the plates was minimized by clamps. The effective width of the tank could be varied by moving two false walls within the gap, the clamps also ensuring that there was no leakage past these walls during bubble motion. In the centre of the base of the tank was a one-way valve, the outlet of which

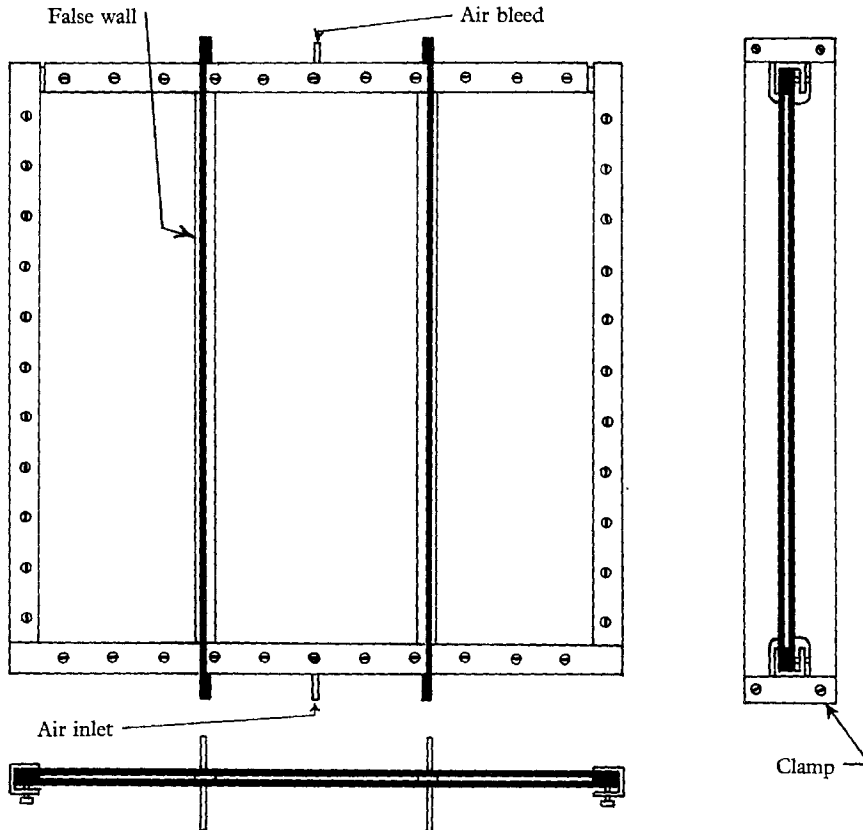


FIGURE 4. Experimental tank.

was covered by two rubber flaps butted over the valve centre line. These ensured a sharp cut-off when air was injected from a hand pump, and produced a bubble with few satellites. With the walls at their widest separation of 33 in., bubble sizes ranged from  $a = 1.5$  in. to  $a = 3.5$  in.

A linen screen ruled with a  $\frac{1}{2}$  in. grid covered one face of the tank and was illuminated uniformly from behind so that the bubble margin appeared dark against this background. A transparent circular protractor rotating at 0.5 rev/sec and also illuminated via the linen screen provided a time scale. Two photographs taken with a 35 mm reflex camera and separated by an interval of approximately 0.5 sec thus provided sufficient information to determine bubble velocity and radius of curvature at the front stagnation point. The latter

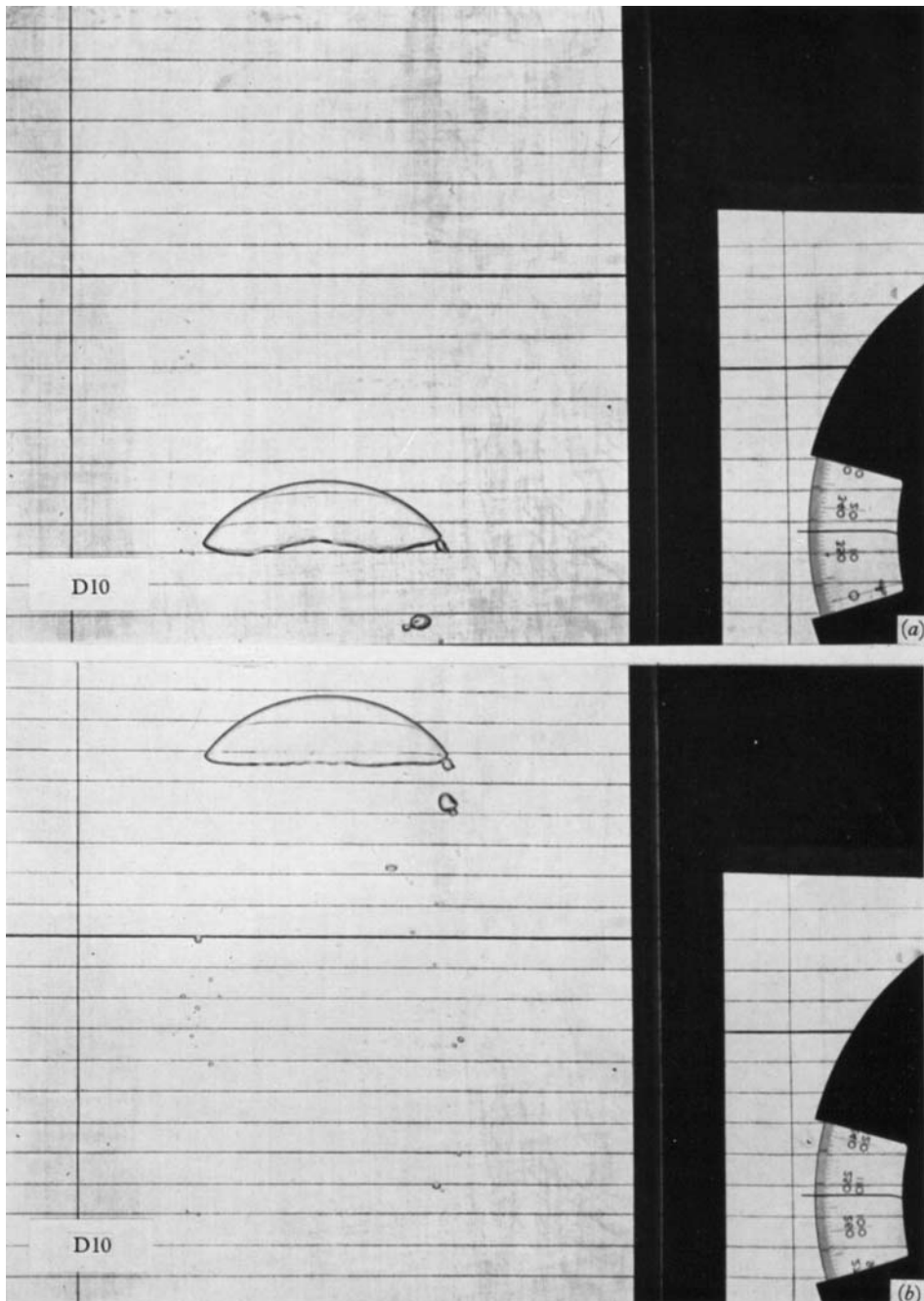


FIGURE 5. A typical pair of photographs,  $a = 2.4$  in.,  $b = 5$  in.,  
 $U = 1.18$  ft. sec.,  $\theta = 110^\circ$ .

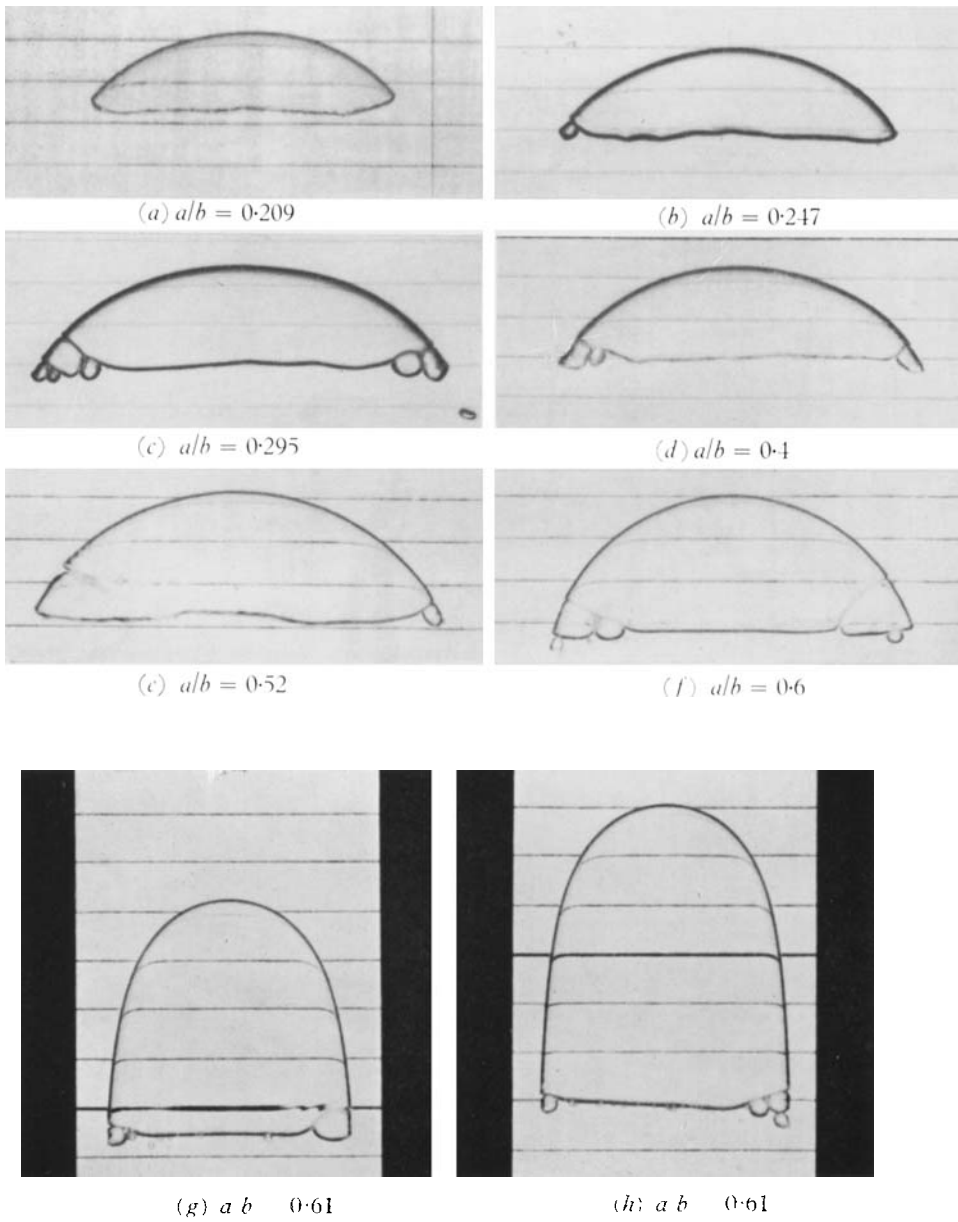


FIGURE 7. Change in bubble shape during transition to the slug form.



measurement was taken by projecting a magnified image of the bubble on a screen and comparing with a standard set of circular arcs. The angle  $\theta$  subtended by the bubble extremities at the centre of curvature was also measured. Due to the change in hydrostatic pressure a bubble expands slightly during its upward motion, so that the mean value of radius of curvature from a pair was taken. By its nature, the method of velocity measurement gave an average value over a distance of approximately 6 in. The initial photograph was taken when the bubble reached the horizontal centre line of the tank; a typical pair is shown in figure 5 (plate 1).

While it is apparent from figure 3 that the predicted variation with  $a/b$  was confirmed, the measured velocities were consistently higher than those given by the model by approximately 9%. Experimental values for the limits were  $U_\infty = 0.545(ga)^{\frac{1}{2}}$ , and  $U_s = 0.35(gb)^{\frac{1}{2}}$  and these were the values used in plotting the experimental points in figure 3. The most likely reason for the discrepancy can be seen in figure 5, in which the inherent three-dimensional character of the bubble is evident from the distortion of the scale through its cap. There was inevitably some flow between the bubble and the faces of the tank and two-dimensional conditions were not produced. In figure 6 the real bubble and a two-dimensional model of the same radius of curvature are compared. The effect of the flow down the tank faces is slightly to reduce the velocity at a point such as  $A$  on the stagnation streamline below the value it would have had at the corresponding point  $A'$  on the two-dimensional model. If the velocity distribution near the stagnation point on the stagnation streamline retains the same form\* as on the two-dimensional model then the local velocities would be given by

$$q = k_1 U t'(z) / \{f'(z)\}^{\frac{1}{2}},$$

where  $k_1 < 1$ . It follows from equation (19) that, in order to satisfy the constant-pressure condition, the bubble velocity would be  $U = U_{2D}/k_1 > U_{2D}$ , the variation of  $U$  with  $a/b$  remaining unchanged. An increase in bubble velocity of 9% would require a reduction in local velocities of only 8%. A paradox now arises. The two-dimensional theory should also apply to the flow in a vertical plane normal to the tank faces and through the stagnation point. On this basis the bubble velocity should be  $U = (gd/3\pi)^{\frac{1}{2}}$  where  $2d$  is the gap width separating the tank faces. In this apparatus  $d = \frac{1}{8}$  in. so that this velocity is much lower than any measured velocity, and exhibits no variation with  $a/b$ . The paradox is resolved by an extension of the previous argument. If the local velocities on the streamline  $SE$  are reduced only slightly by the presence of flow on  $SF$  then conversely, local velocities on  $SF$  would be very greatly reduced below two-dimensional values by the presence of flow on  $SE$ . Assuming the velocity distribution near the stagnation point on  $SF$  to be given by an equation of the form of equation (10) with  $b$  replaced by  $d$ , the multiplying constant  $k_2$  needed in this case would be such that  $k_2 \ll 1$ . It follows again from equation (19) that in order to satisfy the constant pressure condition,  $U = (gd/3\pi)^{\frac{1}{2}}/k_2 \gg (gd/3\pi)^{\frac{1}{2}}$ . The bubble presumably adjusts its shape, and hence  $k_1$  and  $k_2$  so that the constant pressure condition can be satisfied simultaneously on  $SF$  and  $SE$  at the same bubble velocity. When

\* This assumption preserves the two-dimensional variation of  $U$  with  $a/b$  as the experiments confirm.

the bubble fills the channel and forms a slug  $k_1$  and  $k_2$  will be determined by the aspect ratio of the channel cross-section  $b/d$ . From the preceding argument the effect of flow down the tank faces would be expected to be more significant at low aspect ratios, and this is confirmed by experimental results for slugs in tubes of rectangular cross-section 4 in.  $\times$  1 in. reported by Birkhoff & Carter. They gave  $U = 0.41(gb)^{\frac{1}{2}}$  which is 25% above their own theoretical result. Their aspect ratio of 4 should be compared with the minimum of 10 used in the present experiments.

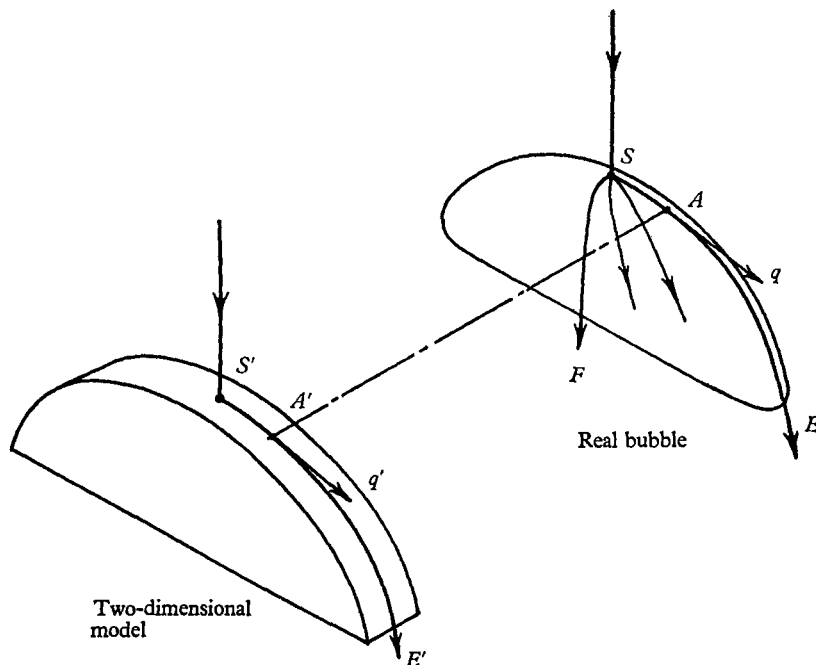


FIGURE 6. Comparison of the real bubble with a two-dimensional model.

A second feature of figure 3 is that the maximum value of  $a/b = 0.955$  allowed by the model was not realized physically, the maximum observed value being 0.64. While this must be regarded as a deficiency, it should be noted also from figure 3 that transfer of control from bubble dimension to channel dimension is virtually complete for values of  $a/b > 0.7$ ; at  $a/b = 0.7$ ,  $U = 0.32(gb)^{\frac{1}{2}}$ , which is less than 2% below its limiting value. A series of photographs depicting transition from the cylindrical-capped form to the slug form is reproduced in figure 7 (plate 2) which shows also the remarkably circular appearance of the cap for values of  $a/b$  below 0.5. Like their three-dimensional counterparts, two-dimensional slugs were found to be geometrically similar near their stagnation points, and the velocity of a slug in a given channel was independent of its length. Despite the high scatter, produced because of the difficulty in defining bubble extremity when a satellite is attached as in figure 7(c), figure 8 indicates how the measured angle subtended at the centre of curvature of the stagnation point changes during transition to the slug form. In an infinite liquid this angle is approximately  $105^\circ$ , while Davies & Taylor found angles of approximately

100° for the spherical-capped bubble. The two-dimensional slug appears to assume a limiting value of  $a/b = 0.62$  in figure 8. Birkhoff & Carter quote a value of  $\sim 0.7$  for the rectangular tube of aspect ratio 4.

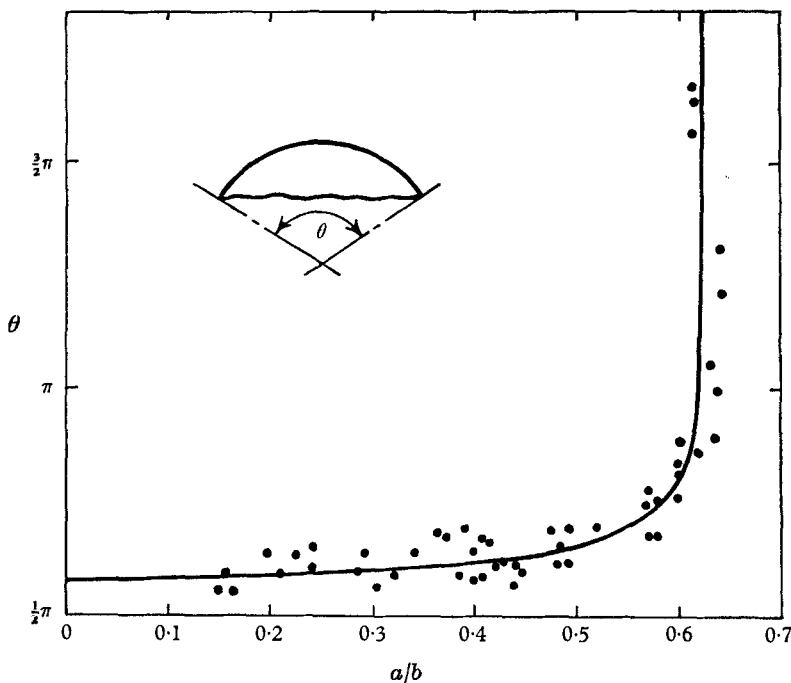


FIGURE 8. Variation of measured included angle with  $a/b$ .

#### 4. Concluding remarks

Although it appears to be impossible to generate a bubble which is truly two-dimensional, the variation of velocity with  $a/b$  determined experimentally was described well by equations (21) and (22). The three-dimensional character of the real flow caused experimental values of velocity to be 9% higher than those given by the two-dimensional model.

The author is indebted to Mr D. R. Allen of the Department of Mechanical Engineering, University College London, for his photographic skill.

#### REFERENCES

- BIRKHOFF, G. & CARTER, D. 1956 *Los Alamos Sci. Lab. Rep.* LA-1927.  
 COLLINS, R. 1965 *Chem. Engng Sci.* (To be published.)  
 DAVIDSON, J. F. 1961 *Trans. Inst. Chem. Engrs*, **39**, 230.  
 DAVIDSON, J. F. & HARRISON, D. 1963 *Fluidized Particles*. Cambridge University Press.  
 DAVIES, R. M. & TAYLOR, G. I. 1950 *Proc. Roy. Soc. A*, **200**, 375.  
 DUMITRESCU, D. T. 1943 *Z. angew. Math. Mech.* **23**, 139.  
 GARABEDIAN, P. R. 1957 *Proc. Roy. Soc. A*, **241**, 423.  
 LAMB, H. 1932 *Hydrodynamics*, 6th ed., p. 71. Cambridge University Press.  
 NICKLIN, D. J., WILKES, J. O. & DAVIDSON, J. F. 1962 *Trans. Inst. Chem. Engrs*, **40**, 61.  
 UNO, S. & KINTNER, R. C. 1956 *A.I.Ch.E.J.* **2**, 420.